Journal of Orthopaedic Translation 28 (2021) 100–107

Contents lists available at ScienceDirect

Journal of Orthopaedic Translation

journal homepage: www.journals.elsevier.com/journal-of-orthopaedic-translation

Treatment of collagen-induced arthritis rat model by using Notch signalling inhibitor

Jianhai Chen [a,b], Jian Li [a,b], Jinqing Chen [c], Wenxiang Cheng [a], Jietao Lin [a,b], Liqing Ke [a], Gang Liu [e], Xueling Bai [a], Peng Zhang [a,b,d,e,*]

[a] Center for Translational Medicine Research and Development, Shenzhen Institutes of Advanced Technology, Chinese Academy of Sciences, Shenzhen, Guangdong, 518055, China
[b] University of Chinese Academy of Sciences, Beijing, 100049, China
[c] Research Laboratory for Biomedical Optics and Molecular Imaging, Shenzhen Key Laboratory for Molecular Imaging, Guangdong Provincial Key Laboratory of Biomedical Optical Imaging Technology, CAS Key Laboratory of Health Informatics, Shenzhen Institutes of Advanced Technology, Chinese Academy of Sciences, Shenzhen, 518055, China
[d] Shenzhen Engineering Research Center for Medical Bioactive Materials, China
[e] Shenzhen Hospital, University of Chinese Academy of Sciences, China

ARTICLE INFO

Keywords:
Rheumatoid arthritis
Notch signalling
Notch signalling signalling
Collagen-induced arthritis

ABSTRACT

Background: The Notch signalling pathway has been reported to play a key role in rheumatoid arthritis (RA) development. Thus, inhibition of the activation of this signalling pathway may be a promising approach to the treatment of RA. In this study, the Notch signalling inhibitor LY411575, which can inhibit both Notch1 and Notch3, was used for the treatment of collagen-induced arthritis (CIA) rats.

Methods: Wistar rats were immunised with bovine type II collagen (CII) to establish rats CIA model. The inhibitory effects of LY411575 on Notch1 intracellular domain (N1ICD) and Notch3 intracellular domain (N3ICD) protein was verified by western blot (WB) *in vitro*. CIA rats were treated with different doses of LY411575 for 15 and 28 days, respectively. Methotrexate and sodium carboxymethyl cellulose (CMC-Na) were used as positive and negative (vehicle) control respectively. Destruction of the rat ankle joint and the bone loss on the periarticular side were evaluated by micro-computed tomography (Micro-CT). In addition, destruction of the ankle articular cartilage and the osteoclast numbers were determined by histology. Expression of N1ICD and N3ICD in the ankle joint was detected by immunohistochemistry.

Results: LY411575 could significantly inhibit the expression of N1ICD and N3ICD *in vitro*. Micro-CT test showed that the ankle joint destruction significantly improved after treatment with LY411575 (5 mg/kg and 10 mg/kg, respectively). The bone quality in the LY411575 (5 mg/kg and 10 mg/kg, respectively) groups were improved compared with the vehicle group. Histological analysis showed that LY411575 (5 mg/kg and 10 mg/kg, respectively) treatment reduced the severity of ankle joint inflammation in CIA rats (including ankle joint destruction, pannus formation, and cartilage damage) and reduced the expression of N1ICD and N3ICD in CIA rats ankle joints significantly.

Conclusion: The inhibitor of Notch signalling LY411575 is an effective treatment for CIA.

The translational potential of this article: Our study provides new evidence to support the potential clinical application of Notch signalling pathway inhibitor LY411575 as a drug candidate for the treatment of RA.

1. Introduction

Rheumatoid arthritis (RA) is a chronic autoimmune disease involving synovial hyperplasia and articular cartilage destruction [1,2]. Currently, many drugs are used to treat RA; however, most of these drugs have exhibit effects after long term use. Therefore, identifying new drug targets for RA has become particularly important. In RA pathological process, the lining cells could form a pannus that invades the adjacent

*Corresponding author. Center for Translational Medicine Research and Development, Shenzhen Institutes of Advanced Technology, Chinese Academy of Sciences, Shenzhen, Guangdong, 518055, China.
E-mail address: peng.zhang@siat.ac.cn (P. Zhang).

https://doi.org/10.1016/j.jot.2021.01.003
Received 25 August 2020; Received in revised form 22 November 2020; Accepted 15 January 2021

articular cartilage and subchondral bone at the boundary of the RA joint [3]. Therefore, the formation of pannus is an important pathological feature of RA, which is accompanied by the whole pathogenesis of RA [4]. Moreover, the pannus has long been considered as an attractive therapeutic target for RA [5,6], and many studies have shown that Notch is the main signalling pathway regulating pannus formation during the pathogenesis of RA [7,8].

It is well known that Notch signalling pathway regulates cell development, differentiation, proliferation, survival, and apoptosis [9,10]. Mammalian cells, there are mainly four Notch receptors (Notch1/2/3/4) and five Notch ligands (Delta-like (DLL)-1, DLL-3, DLL-4, Jagged1, and Jagged2), all of which are transmembrane proteins. The activation of Notch signalling occurs via ligand and receptor binding, followed by the activation of the γ-secretase complex in the membrane and the release of the Notch intracellular domain into the nucleus for transcription [11]. Notch1, Notch2, and Notch3 were mainly expressed in RA synovium [12]. Another report indicated that in RA fibroblast-like synovial cells (RA-FLSs), TNF-α can induce the expression of Notch1, which leads to cell proliferation [13]. For another side recent studies have shown that Notch3 plays an important role in angiogenesis and cartilage destruction in RA [14]. Altogether, the Notch signalling pathway may be a new drug target for the treatment of RA; in particular, Notch1 and Notch3 potentially play key roles in mediating the effect of Notch signalling pathway in the pathology of RA. Our hypothesis is that inhibit the expression of Notch1 and Notch3 may attenuate the development of RA. In this research, the inhibitor LY411575 of the Notch1 and Notch3 intracellular domain (N1ICD and N3ICD) was utilized for the treatment of collagen-induced arthritis (CIA) model and the results were analysed as well.

2. Materials and methods

2.2. Cells culture

MH7A cells were obtained from the Riken Cell Bank (Tsukuba, Japan). They were cultured in the Roswell Park Memorial Institute (RPMI) 1640 medium (Hyclone, Thermo Fisher Scientific, Wilmington, DE, USA), with 10% foetal bovine serum (Gibco, Thermo Fisher Scientific), and 1% penicillin/streptomycin (Sigma–Aldrich, MO, USA). Cell lines were cultured in an incubator at the constant temperature of 37 °C, constant relative humidity, and 5% CO_2.

2.3. Assessment of cell viability

The viability of MH7A cells was assessed using Cell Counting Kit-8 (CCK-8) (Dojindo, Japan). MH7A cells were cultivated in 96-well plates (4000 cells/well) for 24 h and subsequently treated with various concentrations of LY411575 (TOPSCIENCE, USA) for 24 h. Afterwards, 10 μl of the CCK-8 solution was added to each well, ensuring that the volume of CCK-8 was 10% of the volume of medium. The 96-well plate was placed at 37 °C for 1 h; absorbance was measured at 450 nm using a microplate reader (PerkinElmer, Waltham, MA). Cytotoxicity of LY411575 was expressed as the relative viability (%) against the untreated control (culture medium), which represented 100% viability.

2.4. Western blot

MH7A cells were seeded into 6-well plates (1×10^6 cells/well) for 24 h. Cells were lysed in Radio-Immunoprecipitation Assay (RIPA) (Thermo Scientific, USA) lysis and extraction buffer in a cold environment. Afterwards, the lysed cells and lysis buffer were collected in a tube and centrifuged at 12,000 rpm for 25 min, to remove the cell fragments. The protein concentration was measured using the bicinchoninic acid (BCA) kit (Thermo Fisher Scientific, USA), and then the protein was heated with sodium dodecyl sulphate-polyacrylamide gel electrophoreses sample-loading buffer (Beyotime Institute of Biotechnology, Haimen, China) to denature the protein. Protein samples were resolved on an SDS-PAGE system and transferred onto PVDF membranes (Millipore, Co, Bedford, MA). Membranes were blocked in a wash buffer containing 5% non-fat dry milk with gentle agitation for 1 h h at room temperature and then incubated with specific antibody solution at 4 °C overnight. N1ICD antibody (1:500, ab83232, Abcam); N3ICD antibody (1:500, sc-515,825, STAN); P–NF-kappa B–P65 antibody (1:1000, #3033, CST); ICAM-1 (1:1000, #67836, CST) and GAPDH antibody (1:2000, ab8245, Abcam). Polyvinylidene fluoride membrane was washed in Phosphate Buffered Saline Tween (PBST) (Sigma–Aldrich) to remove redundant antibody structures; then, the membrane was incubated with the corresponding secondary antibody at room temperature for 1 h. An enhanced Electrochemiluminescence (ECL) system was used to detect antibody binding. The results were quantified using GelView 6000Plus System (Shanghai, China).

2.5. Animals

Eighty male Wistar rats 10 weeks of age were purchased from Beijing Vital River Laboratory Animal Technology Co., Ltd (China). The rats were maintained in a specific pathogen-free (SPF) facility. The rat study protocols were approved by the animal ethical and welfare committee of the Shenzhen Institutes of Advanced Technology, Chinese Academy of Sciences (SIAT-IACUC-190723-KYC-ZP-A0804).

2.6. The experimental group

Immunization grade bovine type II collagen (Chondrex, USA) was emulsified with an equal volume of incomplete Freund's adjuvant. On day 0, 0.2 mL of the emulsion was subcutaneously injected into the tail base of the treatment group rats, followed by a booster injection on day 7. Treatment group rats were given oral gavage once a day. After administration, six rats in each group were selected for each efficacy index on days 15th and 28th.

Sodium carboxymethyl cellulose (CMC-Na) was used as a vehicle for drug and control treatments. After the onset of arthritis, the rats were divided into the following six groups (n = 12); normal (CMC-Na); vehicle-treated (CIA with CMC-Na); methotrexate (MTX)-treated [(CIA with 0.2 mg/kg by weight (bw)]; low concentration (CIA with 1 mg/kg bw) LY411575-treated group; medium concentration (CIA with 5 mg/kg bw) LY411575-treated group; high concentration (CIA with 10 mg/kg bw) LY411575-treated group. Rats were administered the treatments by oral gavage once a day, and six rats from each group were tested for treatment efficacy on days 15 and 28, respectively.

2.7. Micro-CT

At different time points (on days 15th and 28th) after treatment, micro-CT (Sky-Scan, Bruker, Belgium) analyses were performed on the ankle joint. Samples were imaged with an X-ray tube voltage of 50 kV and current of 400 μA, with a 0.1 mm Cu filter. The scanning angular rotation was 180°, and the angular increment was 0.90°. Reconstruction and analysis were performed automatically. Each sample was scanned using a Hounsfield unit supplied with a micro-CT scanner. Joint bone radiological destruction was scored on a scale from 0 to 3: 0, no damage; 1, minor; 2, moderate; 3, severe [15]. The ankle joint was selected for bone volume to tissue volume (BV/TV) and trabecular number (Tb. N).

2.8. Histological analysis

Overdose of sodium pentobarbital euthanized the rats. The rat ankle joint samples were fixed in cold paraformaldehyde solution (4%) for 48 h, and then decalcified in 0.5 M EDTA solution for 70 days. Then, the ankle joint was embedded in paraffin and a paraffin section (5-μm thick) was used for histological analysis. Haematoxylin-Eosin (H&E) staining kit (Beyotime, China), Safranine O-Fast Green (Solarbio, China), and

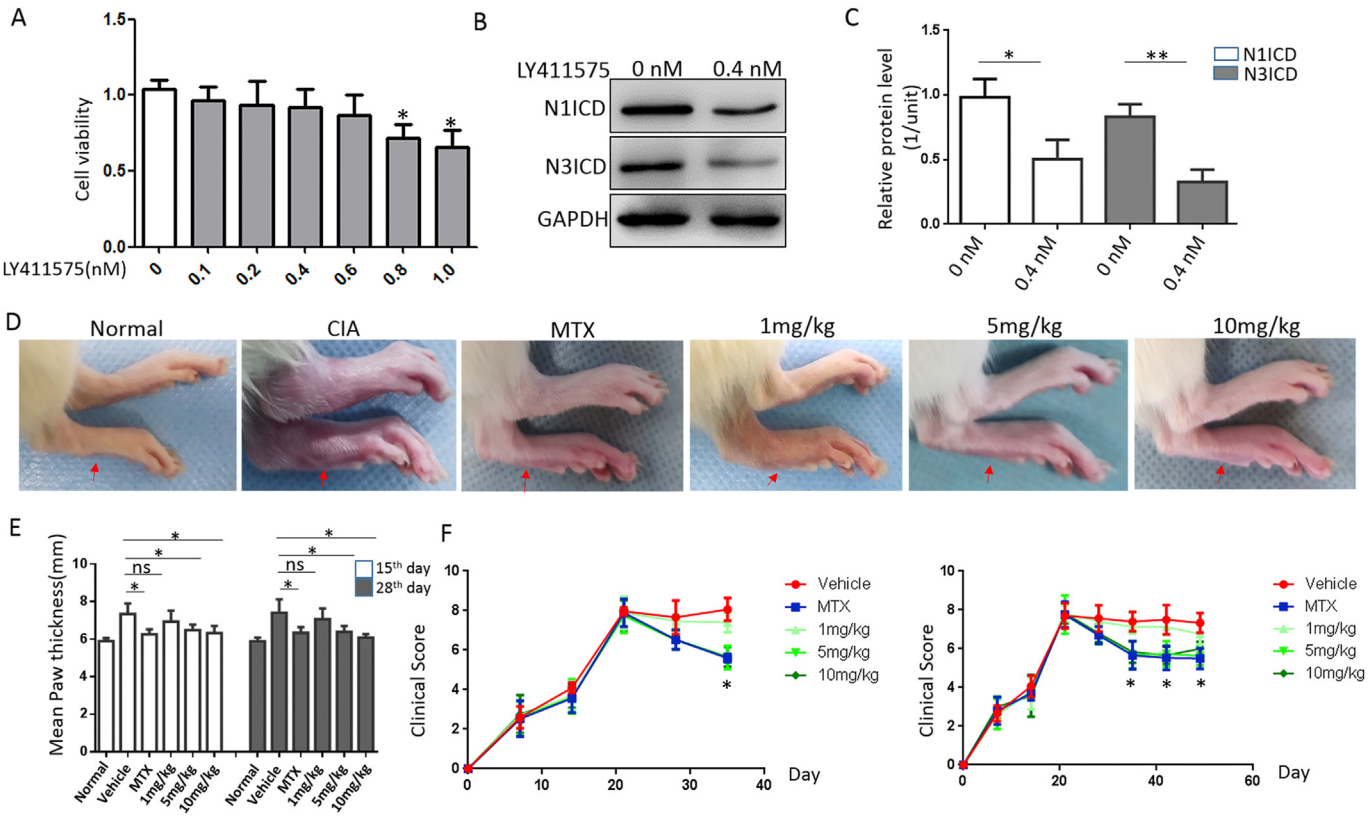

Fig. 1. Cytotoxicity of LY411575 on MH7A cells and macroscopic observation of joint swelling in rats with CIA (A) Cytotoxicity of LY411575 (0, 0.1, 0.2, 0.4, 0.6, 0.8 nM) on MH7A cells (*P < 0.05, n = 3, versus control) (B)Western blot result of N1ICD and N3ICD expression after using LY411575 (0.4 nM) (C) Semi-quantitative WB (*P < 0.05, **P < 0.01, n = 3) (D) Paw photos of CIA rats were taken after treatment (E) Paw thickness at the end of treatment (n = 6) (F) Arthritis scores were monitored once every 7 days.

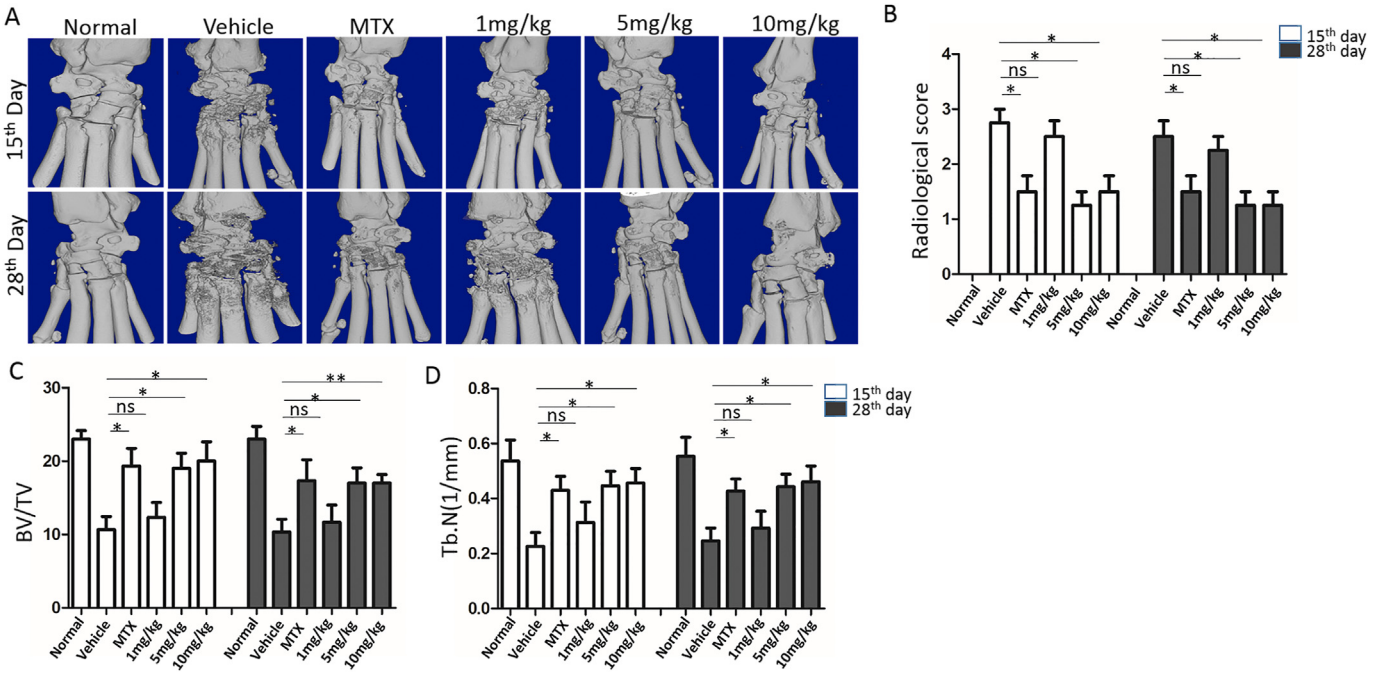

Fig. 2. Micro-CT analyses after 15th and 28th days of drug administration to assess joint destruction and semi-quantitative integration statistics (A) Representative 3D reconstructions of micro-CT images of the ankle joint (B) Radiological score (C) Ratio of bone volume to tissue volume (BV/TV) (D) Trabecular number (Tb. N) (*P < 0.05, **P < 0.01, n = 6).

TRAP (Sigma, USA) staining were performed according to standard protocols, respectively. After staining, we observed the pathological changes in tissues under an optical microscope. H&E scored [16] from 0 to 4; 0, normal joint synovial tissue and bone structure; 1, synovial cell

hypertrophy and inflammatory cell erosion of synovial tissue; 2, cartilage destruction and pannus present; 3, most articular cartilage and subchondral bone are destroyed; 4, joint adhesions and stiffness and accompanying disability. Toluidine Blue scored [17] from 0 to 3, where: 0, normal; 1, slight cartilage erosion; 2, moderate cartilage erosion; 3, severe cartilage erosion or bone destruction. The number of TRAP-positive cells was quantified.

2.9. Immunohistochemical analysis

Immunohistochemical staining for N1ICD and N3ICD proteins was completed. Paraffin-fixed sections were repaired with an antigen boiling in 1% citrate buffer for 15 min, and incubated in 0.3% hydrogen peroxide for 10 min at room temperature to block endogenous peroxidase activity. Then, they were incubated in a protein-free blocking buffer at room temperature for 10 min to block background non-specific staining. We followed the operating instructions for the HRP/DAB (ABC) Detection IHC Kit (ab64264, Abcam). Mean optical density (MOD) was calculated to analyse the semi-quantitative expression of N1ICD and N3ICD using Image-Pro plus 6.0 software.

2.10. Statistical analysis

Prism *v.7.0* (GraphPad Software, San Diego, California, USA) was used for the analysis. One-way analysis of variance was used for multiple group analysis. The two-tailed unpaired t-test was used to analyze the data from two groups. P values of less than 0.05 and 0.01 were considered significant.

3. Results

3.1. Verification of the effect of Notch signalling inhibitor in vitro and animal model in vivo

To determine the optimal concentration of LY411575, CCK-8 was used to detect the viability of MH7A cells treated with different concentrations of LY411575. The results shown that there were no significant difference between 0.1 and 0.6 nmol/L and 0 nmol/L, while 0.8 nmol/L and 1.0 nmol/L are significantly different from 0 nmol/L (Fig. 1A). These results indicated that the inhibitor LY411575 had no effect on the viability of MH7A cells in the concentration ranges up 0–0.6 nmol/L. Based on the results of the cell viability test, LY411575 was used at a concentration of 0.4 nmol/L to treat MH7A cells for a subsequent experiment. The results showed that the protein expressions of N1ICD and N3ICD were significantly inhibited by LY411575 (Fig. 1B and C).

RA symptoms were observed in 47 of 55 immunised rats, one week after the second immunization. Compared with vehicle group, ankle redness and swelling (Fig. 1D and E) and the clinical score (Fig. 1F) were significantly lower after treatment with LY411575 (5 mg/kg and 10 mg/kg) and MTX.

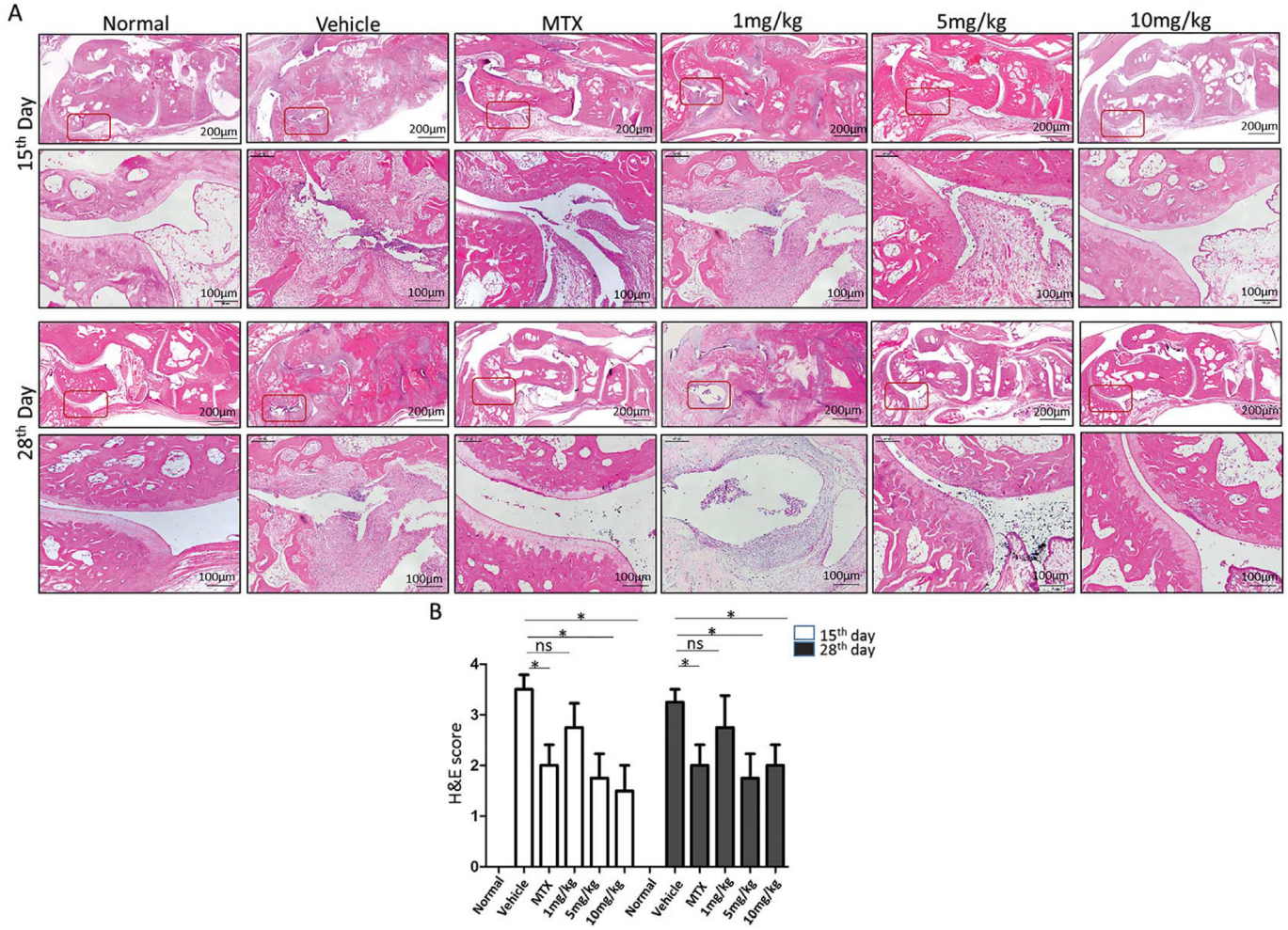

Fig. 3. H&E staining results after 15th and 28th days of treatment (A) H&E stains the ankle joint (B) H&E semi-quantitative score (*P < 0.05, ns = not significant, n = 6).

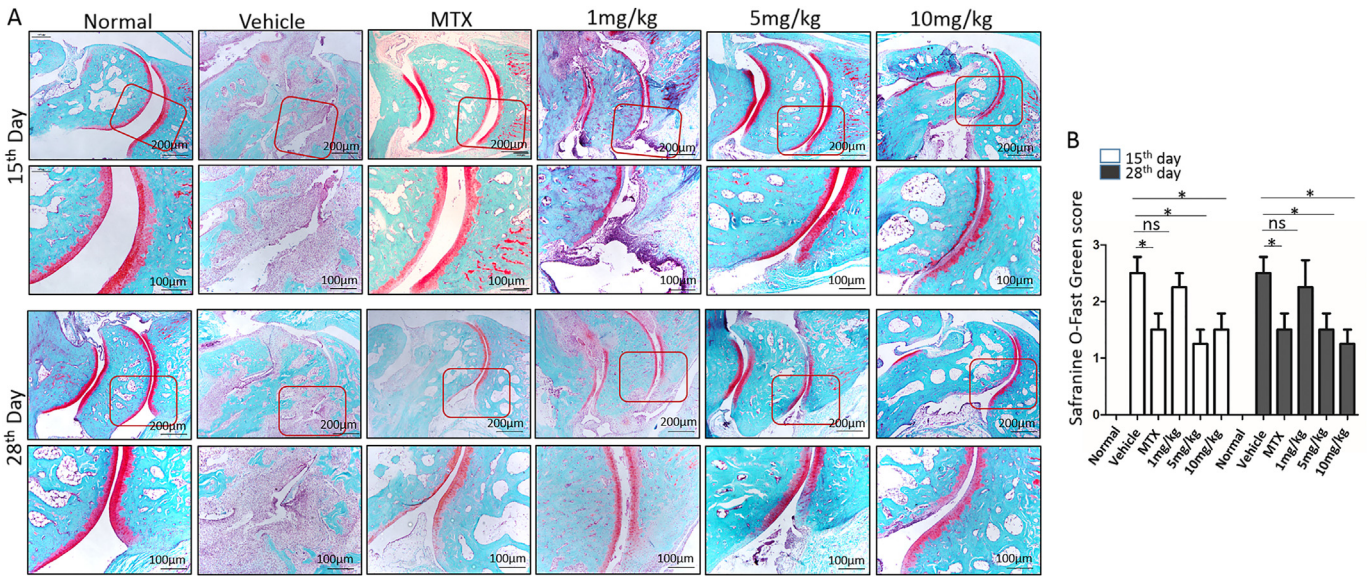

Fig. 4. Toluidine blue analysis of cartilage destruction after 15th and 28th days of treatment (A) Toluidine blue staining (B) Cartilage destruction scores (*P < 0.05, ns = not significant, n = 6).

3.2. Micro-CT observation

Pathological changes in the ankle joints of in rats were analysed by micro-CT after 15th and 28th days of treatment. Results showed that articular bone destruction was clearly visible in the vehicle group compared with the normal group. The ankles of the rats injected with LY411575 (5 mg/kg and 10 mg/kg) group and the MTX group showed significantly improved cartilage and joints compared with the vehicle group. No significant differences were observed between the LY411575 (1 mg/kg) group and the vehicle groups, indicating that the effects of LY411575 were dose dependent (Fig. 2A and B). Quantitative analysis of BV/TV after 15 days of treatment showed that the values were 1.87- and 1.76-fold higher in the LY411575 (5 and 10 mg/kg) groups, respectively, and 1.82-fold higher in the MTX group than those in the vehicle group. After 28 days of treatment, the BV/TV values were 1.83- and 1.77-fold higher in the LY411575 (5 and 10 mg/kg) groups, respectively, and 1.86-fold higher in the MTX group than those in the vehicle group (Fig. 2C). Quantitative analysis of Tb.N after 15 days of treatment showed that the values were 1.95- and 2.09-fold higher in the LY411575 (5 and 10 mg/kg) groups, respectively, and 1.93-fold higher in the MTX group than those in the vehicle group. After 28 days of treatment, the Tb.N values were 1.87- and 1.91-fold higher in the LY411575 (5 and 10 mg/kg) groups, respectively, and 1.79-fold higher in the MTX group than those in the vehicle group (Fig. 2D).

3.3. Histological analyses

Haematoxylin and eosin (H&E) staining was used to analyse the improvement in the ankle joint after treatment. The results showed significant inflammatory cell infiltration and ankle articular cartilage damage in the vehicle group compared with those in the normal group. Compared with the vehicle group after 15th and 28th days of

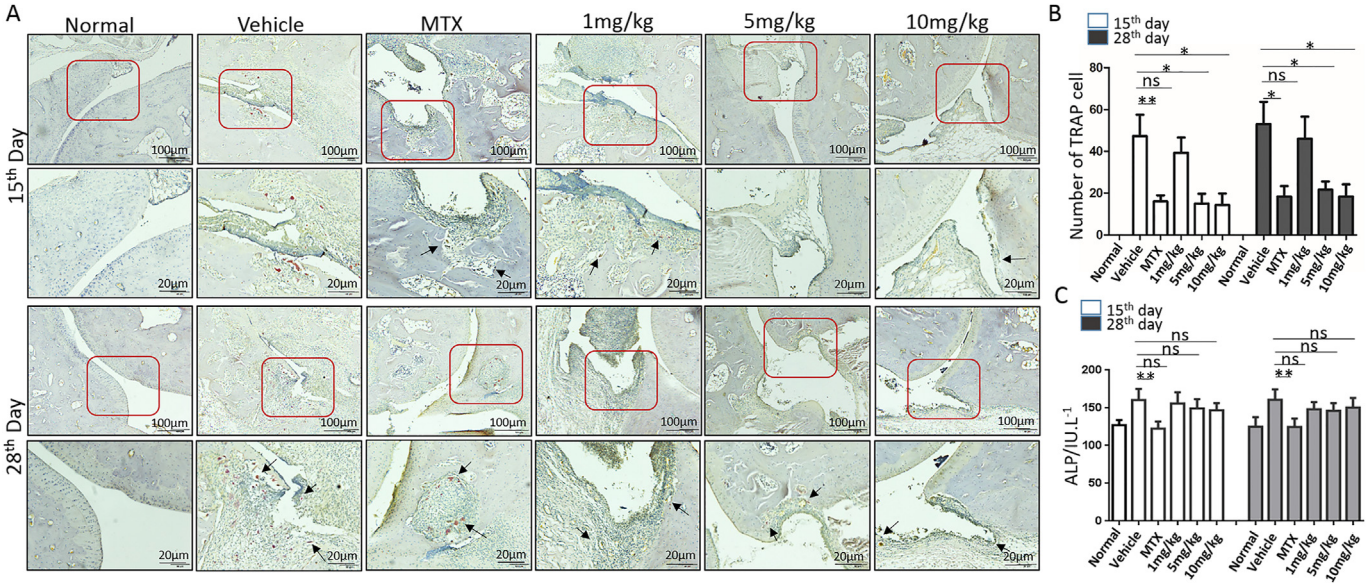

Fig. 5. Tissue sections were stained with TRAP after 15th and 28th days of treatment (A) TRAP-positive osteoclasts were stained red (B) The number of TRAP positive cells were counted (*P < 0.05, **P < 0.01, ns = not significant, n = 6) (C) The expression of ALP in serum.

administration, the LY11575 (5 and 10 mg/kg) group and MTX group inflammatory cell infiltration and cartilage damage were improved, but no significant improvement was found in the 1 mg/kg group (Fig. 3A). Quantitative analysis showed that after 15 days of treatment, the H&E scores were 1.60- and 1.77-fold lower in the LY411575 (5 and 10 mg/kg) groups, respectively, and 1.94-fold lower in the MTX group than those in the vehicle group. After 28 days of treatment, the H&E scores were 1.70- and 1.66-fold lower in the LY411575 (5 and 10 mg/kg) groups, respectively, and 2.26-fold lower in the MTX group than those in the vehicle group (Fig. 3B).

Cartilage damage was analysed using safranine O/fast green staining of the ankle joint. The results showed that the ankle joint cartilage was severely damaged in the vehicle group, and no cartilage was found after 28 days. After 15 and 28 days of administration, the LY411575 (5 and 10 mg/kg) and MTX groups showed reduced cartilage damage compared with that in the vehicle group, while no significant improvement was observed in the LY411575 (1 mg/kg) group (Fig. 4A). Quantitative analysis showed that after 15 days of treatment, the safranine O/fast green scores were 2.09- and 1.79-fold lower in the LY411575 (5 and 10 mg/kg) groups, respectively, and 2.14-fold lower in the MTX group than those in the vehicle group. After 28 days of treatment, the safranine O/fast green scores were 2.15- and 3.63-fold lower in the LY411575 (5 and 10 mg/kg) groups, respectively, and 1.89-fold lower in the MTX group than those in the vehicle group (Fig. 4B).

Tartrate-resistant acid phosphatase (TRAP) staining was used to analyse the number of positive osteoclast cells. The results showed large numbers of osteoclasts in the ankle joints of rats from the vehicle group compared with those in the normal group. Compared with the vehicle group, the LY411575 (5 and 10 mg/kg) and MTX groups exhibited significantly reduced numbers of osteoclasts after 15 and 28 days of administration; however, no significant reduction was observed in the LY511575 (1 mg/kg) group (Fig. 5A). After 15 days of treatment, the TRAP-positive cell counts were 3.15- and 3.37-fold lower in the LY411575 (5 and 10 mg/kg) groups, respectively, and 2.95-fold lower in

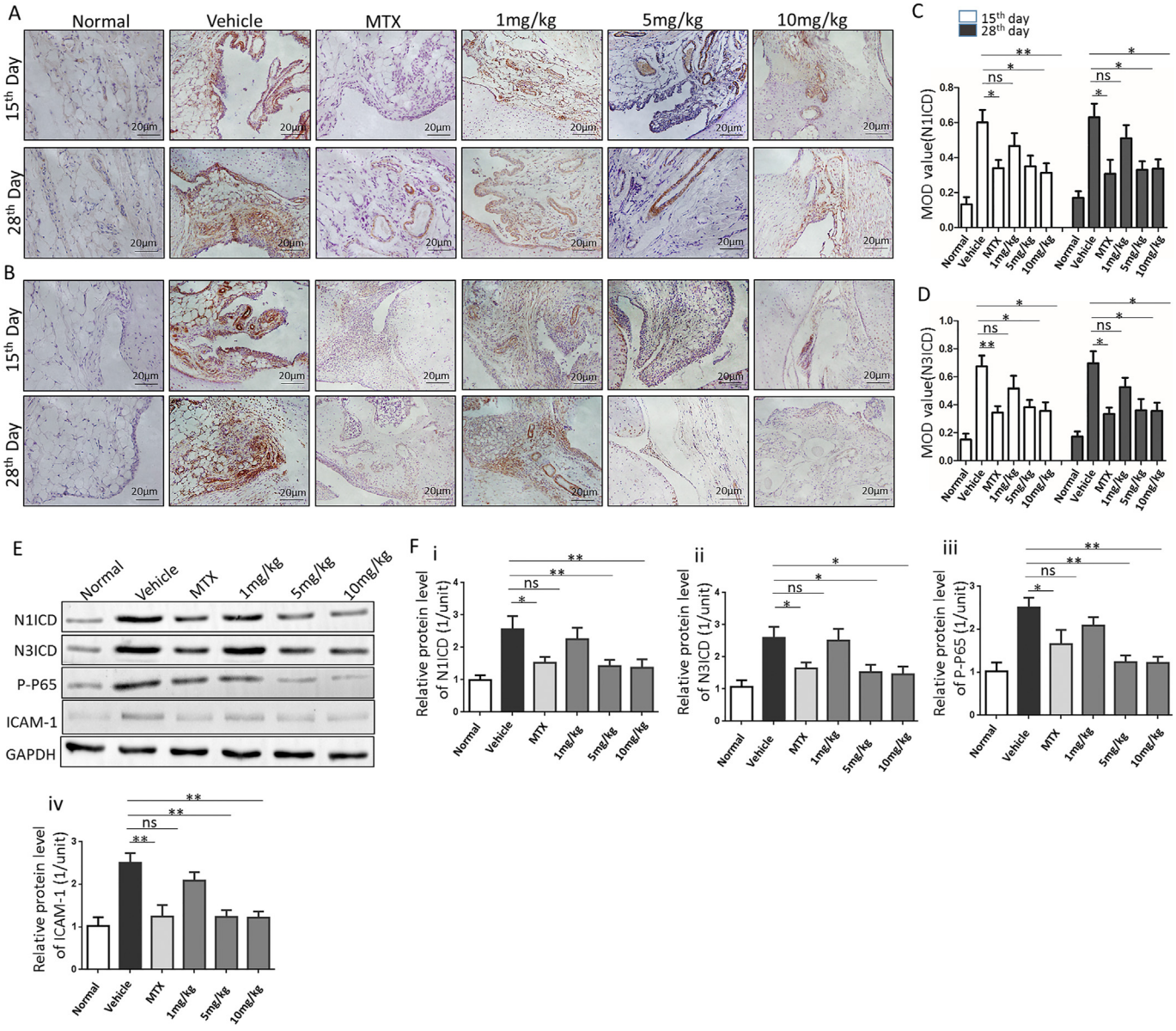

Fig. 6. The results of immunohistochemical staining were after 15th days and 28th days of treatment (A) Immunohistochemical staining results for N1ICD (B) Immunohistochemical staining results for N3ICD (C) Quantitative immunohistochemical results for N1ICD expressed as mean optical density (MOD) values (D) Quantitative immunohistochemical results for N3ICD expressed as MOD values (*P < 0.05, **P < 0.01, ns = not significant, n = 6) (E) WB result of N1ICD, N3ICD, P–NF-κB-P65 and ICAM-1 in ankle (F) Semi-quantitative WB (*P < 0.05, **P < 0.01, n = 3).

the MTX group than those in the vehicle group. After 28 days of treatment, the TRAP-positive cell counts were 2.52- and 2.94-fold lower in the LY411575 (5 and 10 mg/kg) groups, respectively, and 2.39-fold lower in the MTX group than those in the vehicle group (Fig. 5B). The osteogenic marker alkaline phosphatase (ALP) showed no significant differences between the LY411575 treatment groups and the vehicle group (Fig. 5C).

3.4. Immunohistochemical analysis of the protein expressions of N1ICD and N3ICD in vivo

Compared with those in the normal group, the N1ICD (Fig. 6A) and N3ICD (Fig. 6B) expression levels were significantly higher in the ankle joints of rats in the vehicle group. Compared with that in the vehicle group, the expression of N1ICD and N3ICD was significantly reduced in the LY411575 (5 and 10 mg/kg) and MTX groups after 15 and 28 days of administration, but there was no significant decrease in the LY411575 (1 mg/kg) group. After 15 days of treatment, the expression levels of N1ICD were 1.93- and 1.94-fold lower in the LY411575 (5 and 10 mg/kg) groups, respectively, and 1.76-fold lower in the MTX group than those in the vehicle group. After 28 days of treatment, the expression of N1ICD was 1.91- and 1.87-fold lower in the LY411575 (5 and 10 mg/kg) groups, respectively, and 2.01-fold lower in the MTX group than that in the vehicle group (Fig. 6C). The MOD of N3ICD expression in positive cells revealed that after 15 days of treatment, the expression levels of N3ICD were 1.76- and 1.91-fold lower in the LY411575 (5 and 10 mg/kg) groups, respectively, and 1.97-fold lower in the MTX group than those in the vehicle group. After 28 days of treatment, the expression levels of N3ICD were 2.39- and 2.73-fold lower in the LY411575 (5 and 10 mg/kg) groups, respectively, and 2.86-fold lower in the MTX group than those in the vehicle group (Fig. 6D). To further analyse the protein expression in the ankle joints and synovial tissue after LY411575 treatment. After 15 days of treatment, we determined the expression levels of N1ICD and N3ICD, as well as those of the proinflammatory signalling pathway proteins P–NF- kappa B–P65 and intercellular adhesion molecule 1 (ICAM-1). The results showed that after treatment with LY411575 (5 and 10 mg/kg), the expression levels of N1ICD (Fig. 6E and F-i), N3ICD (Fig. 6E and F-ii), P–NF-κB-P65 (Fig. 6E and F-ii) and ICAM-1 (Fig. 6E and F-iv) were significantly lower than those in the vehicle group.

4. Discussion

Although there are many drugs for RA treatment, few of them can lead to total cure. It has been reported that Notch signalling pathway plays a key role in the pathogenesis of RA [8,19]. Most of the previous studies have focused on Notch1 as the research target [20]. However, it has recently been shown that Notch3 is also involved in RA pathogenesis [14], LY411575 which is the inhibitor of Notch1 and Notch3 has been widely used to inhibit the Notch signalling pathway [21]. Recent studies have reported that LY411575 effectively inhibit osteoclast differentiation, osteoclast-specific gene expression, and angiogenesis [22,23]. To even illustrate the potential therapeutic value in clinics, in this research we observed a significant positive results of LY411575 for the treatment in CIA rats. Similar to a previous study [22], we demonstrated significant positive effects of LY411575 on CIA in rats, which suggests the potential therapeutic value of LY411575. In particular, we found that LY411575 treatment of CIA rats could reduce the positive rate of osteoclasts in the ankle joint but had no significant effect on osteoblast ALP activity.

It has been widely reported that Notch signalling pathway plays a key role in angiogenesis during embryonic development [24]. Moreover, the potential affected of Notch signalling pathway on the immune system has been illustrated [25,26]. Furthermore, Notch signalling plays a key role in the differentiation of peripheral T and B lymphocytes [27,28]. In addition, gene suppression and drug therapy have shown that the blocking of the Notch signalling pathway can reduce the levels of activated NF-κB-P65, ICAM-1, and proinflammatory cytokines in a focal cerebral ischaemia model [30,31].

RA is an immune system disorder that mainly affected the joint and characterized as arthritis [32,33]. Therefore, we hypothesized that the inhibition of Notch signalling may provide new therapeutic effect on RA. Our study indicated that the Notch signalling pathway inhibitor LY411575 can reduce the destruction of articular cartilage (Figs. 2, 4 and 5), pannus formation, inflammatory cell infiltration (Fig. 3), and reduce the expression of pro-inflammatory cytokines p65 in joint synovium (Fig. 6) in CIA rats, which verified our hypothesis strongly.

5. Conclusion

In summary, our results showed that inhibition of Notch signalling using LY411575 could effectively ameliorate the pathological process of CIA in rats. Notch signalling pathway may thus be a new target for the treatment of RA.

Declaration of competing interest

The authors have declared no conflicts of interest.

Acknowledgements

National Key R&D Program of China (2018YFC1705205); Foreign cooperation project of Chinese Academy of Sciences (GJHZ2063); National Natural Science Foundation of China (92068117); Guangdong Basic and Applied Basic Research Fund (2020B1515120052); Science and Technology Innovation Fund of ShenZhen (JCYJ20170818153602439, JCYJ20180302150101316); Sanming Project of Medicine in Shenzhen (SZSM201808072); Development and Reform Commission of Shenzhen Municipality (XMHT20190106001); Development and Reform Commission of Shenzhen Municipality (2019) No. 561. Shenzhen Double Chain Project for Innovation and Development Industry supported by Bureau of Industry and Information Technology of Shenzhen (201908141541).

References

[1] McInnes IB, Schett G. Pathogenetic insights from the treatment of rheumatoid arthritis. Lancet 2017;389(10086):2328–37.
[2] McInnes IB, Buckley CD, Isaacs JD. Cytokines in rheumatoid arthritis - shaping the immunological landscape. Nat Rev Rheumatol 2016;12(1):63–8.
[3] Fassbender HG, Gay S. Synovial processes in rheumatoid arthritis. Scand J Rheumatol Suppl 1988;76:1–7.
[4] Bottini N, Firestein GS. Duality of fibroblast-like synoviocytes in RA: passive responders and imprinted aggressors. Nat Rev Rheumatol 2013;9(1):24–33.
[5] Paleolog EM. Angiogenesis in rheumatoid arthritis. Arthritis Res 2002;4(Suppl 3): S81–90.
[6] Cheng WX, Huang H, Chen JH, Zhang TT, Zhu GY, Zheng ZT, et al. Genistein inhibits angiogenesis developed during rheumatoid arthritis through the IL-6/JAK2/STAT3/VEGF signalling pathway. J Orthop Translat 2020;22:92–100.
[7] Gao W, Sweeney C, Walsh C, Rooney P, McCormick J, Veale DJ, et al. Notch signalling pathways mediate synovial angiogenesis in response to vascular endothelial growth factor and angiopoietin 2. Ann Rheum Dis 2013;72(6):1080–8.
[8] Gao W, Sweeney C, Connolly M, Kennedy A, Ng CT, McCormick J, et al. Notch-1 mediates hypoxia-induced angiogenesis in rheumatoid arthritis. Arthritis Rheum 2012;64(7):2104–13.
[9] Fiuza UM, Arias AM. Cell and molecular biology of Notch. J Endocrinol 2007; 194(3):459–74.
[10] Bray S, Bernard F. Notch targets and their regulation. Curr Top Dev Biol 2010;92: 253–75.
[11] Selkoe D, Kopan R. Notch and Presenilin: regulated intramembrane proteolysis links development and degeneration. Annu Rev Neurosci 2003;26:565–97.
[12] Ishii H, Nakazawa M, Yoshino S, Nakamura H, Nishioka K, Nakajima T. Expression of notch homologues in the synovium of rheumatoid arthritis and osteoarthritis patients. Rheumatol Int 2001;21(1):10–4.
[13] Ando K, Kanazawa S, Tetsuka T, Ohta S, Jiang X, Tada T, et al. Induction of Notch signaling by tumor necrosis factor in rheumatoid synovial fibroblasts. Oncogene 2003;22(49):7796–803.
[14] Wei K, Korsunsky I, Marshall JL, Gao A, Watts GFM, Major T, et al. Notch signalling drives synovial fibroblast identity and arthritis pathology. Nature 2020;582(7811): 259–64.
[15] Jia Q, Wang T, Wang X, Xu H, Liu Y, Wang Y, et al. Astragalin suppresses inflammatory responses and bone destruction in mice with collagen-induced arthritis and in human fibroblast-like synoviocytes. Front Pharmacol 2019;10:94.

[16] Tomita T, Takeuchi E, Tomita N, Morishita R, Kaneko M, Yamamoto K, et al. Suppressed severity of collagen-induced arthritis by in vivo transfection of nuclear factor kappaB decoy oligodeoxynucleotides as a gene therapy. Arthritis Rheum 1999;42(12):2532–42.
[17] Zhu M, Tang D, Wu Q, Hao S, Chen M, Xie C, et al. Activation of beta-catenin signaling in articular chondrocytes leads to osteoarthritis-like phenotype in adult beta-catenin conditional activation mice. J Bone Miner Res 2009;24(1):12–21.
[19] Keewan E, Naser SA. The role of notch signaling in macrophages during inflammation and infection: implication in rheumatoid arthritis? Cells 2020;9(1).
[20] Park JS, Kim SH, Kim K, Jin CH, Choi KY, Jang J, et al. Inhibition of notch signalling ameliorates experimental inflammatory arthritis. Ann Rheum Dis 2015;74(1):267–74.
[21] AlMuraikhi N, Ali D, Vishnubalaji R, Manikandan M, Atteya M, Siyal A, et al. Notch signaling inhibition by LY411575 attenuates osteoblast differentiation and decreased ectopic bone formation capacity of human skeletal (mesenchymal) stem cells. Stem Cell Int 2019;2019:3041262.
[22] Chen X, Chen X, Zhou Z, Qin A, Wang Y, Fan B, et al. LY411575, a potent gamma-secretase inhibitor, suppresses osteoclastogenesis in vitro and LPS-induced calvarial osteolysis in vivo. J Cell Physiol 2019;234(11):20944–56.
[23] Zhu RR, Chen Q, Liu ZB, Ruan HG, Wu QC, Zhou XL. Inhibition of the Notch1 pathway induces peripartum cardiomyopathy. J Cell Mol Med 2020;24(14):7907–14.
[24] Park M, Yaich LE, Bodmer R. Mesodermal cell fate decisions in Drosophila are under the control of the lineage genes numb, Notch, and sanpodo. Mech Dev 1998;75(1–2):117–26.
[25] Radtke F, Fasnacht N, Macdonald HR. Notch signaling in the immune system. Immunity 2010;32(1):14–27.
[26] Maillard I, Adler SH, Pear WS. Notch and the immune system. Immunity 2003;19(6):781–91.
[27] Hoyne GF, Dallman MJ, Champion BR, Lamb JR. Notch signalling in the regulation of peripheral immunity. Immunol Rev 2001;182:215–27.
[28] Jiao Z, Wang W, Guo M, Zhang T, Chen L, Wang Y, et al. Expression analysis of Notch-related molecules in peripheral blood T helper cells of patients with rheumatoid arthritis. Scand J Rheumatol 2010;39(1):26–32.
[30] Cheng P, Zlobin A, Volgina V, Gottipati S, Osborne B, Simel EJ, et al. Notch-1 regulates NF-kappaB activity in hemopoietic progenitor cells. J Immunol 2001;167(8):4458–67.
[31] Espinosa L, Cathelin S, D'Altri T, Trimarchi T, Statnikov A, Guiu J, et al. The Notch/Hes1 pathway sustains NF-kappaB activation through CYLD repression in T cell leukemia. Canc Cell 2010;18(3):268–81.
[32] Choudhary N, Bhatt LK, Prabhavalkar KS. Experimental animal models for rheumatoid arthritis. Immunopharmacol Immunotoxicol 2018;40(3):193–200.
[33] Smolen JS, Aletaha D, McInnes IB. Rheumatoid arthritis. Lancet 2016;388(10055):2023–38.